# Human influence on European winter wind storms such as those of January 2018

Robert Vautard[1], Geert Jan van Oldenborgh[2], Friederike E. L. Otto[3], Pascal Yiou[1], Hylke de Vries[2], Erik van Meijgaard[2], Andrew Stepek[2], Jean-Michel Soubeyroux[4], Sjoukje Philip[2], Sarah F. Kew[2], Cecilia Costella[5], Roop Singh[5], Claudia Tebaldi[6]

[1]Laboratoire des Sciences du Climat et de l'Environnement, UMR 8212 CEA/CNRS/UVSQ, IPSL & U Paris Saclay, Gif-sur-Yvette, France
[2]Royal Netherlands Meteorological Institute (KNMI), De Bilt, Netherlands
[3]Environmental Change Institute, University of Oxford, Oxford, UK
[4]Météo-France, Direction des Services Climatiques, Toulouse, France
[5]Red Cross Red Crescent Climate Centre
[6]National Centre for Atmospheric Research, U. S. A.

*Correspondence to*: Robert Vautard (Robert.vautard@lsce.ipsl.fr)

**Abstract.** Several major storms pounded Western Europe in January 2018, generating large damages and casualties. The two most impactful ones, Eleanor and Friederike, are analysed here in the context of climate change. Near surface wind speed station observations exhibit a decreasing trend of the frequency of strong winds associated with such storms. High-resolution regional climate models on the other hand show no trend up to now and a small increase in the future due to climate change. This shows that that factors other than climate change, which are not represented (well) in the climate models, caused the observed decline in storminess over land. A large part is probably due to increases in surface roughness, as shown for a small set of stations covering The Netherlands and in previous studies. This trend could therefore be independent from climate evolution. We concluded that human-induced climate change has had so far no significant influence on storms like the two studied. However, all simulations indicate that global warming could lead to a marginal increase (0-20%) of the probability of extreme hourly winds until the middle of the century, consistent with previous modelling studies. However, this excludes other factors, such as roughness, aerosols, and decadal variability, which have up to now caused a much larger negative trend. Until these factors are simulated well by climate models they cannot give credible projections of future storminess over land in Europe.

## 1 Introduction

The influence of climate change on extratropical storms has been the subject of a number of studies so far (Ulbrich et al.; 2009). It has been demonstrated that with the expansion of the Hadley Cell the storm tracks are moving poleward (Yin, 2005; Bengtsson and Hodges, 2006; Ulbrich et al., 2008). However conflicting results regarding wind storm intensities have not allowed a clear understanding of expected changes in the evolution of extratropical wind storms. A decreasing trend in

storminess indices has been found in observations (Smits et al., 2005; Wever, 2012), consistent with observed large-scale near-surface wind decreases found over continental areas (Vautard et al., 2010; McVicar et al., 2012). By contrast, A more zonal flow is expected from climate projections (Haarsma et al., 2013), inducing a large-scale environment more favorable to winter wind storms. Over Mid-Northern Europe, along the track of highest mean wind speeds, a slight increase in extreme wind

5    speeds was found in several model studies (Ulbrich et al., 2009; Mölter et al., 2016; Vautard et al, 2014), while no consistent changes were found in wind storms number or intensities over the Mediterranean areas (Nissen et al., 2014). The frequency of occurrence of "sting jets", sometimes found in the strongest wind storms in the North-East Atlantic has been suggested to be increasing, from climate model simulations (Martinez-Alvarado et al., 2018), but the concerned area is mostly over ocean.

10   While storms change have been studied as a category, only few event attribution studies analyzed the influence of human activities on extratropical wind storms. There are few other studies on observed trends in wind storms over Europe and these results were mostly inconclusive. Vose et al. (2014) call trends over land "inconclusive", but find a trend over sea. Barredo (2015) finds no upward trend in losses indicating insignificant storminess change. Beniston (2007) finds a sharp decline in wind storms in Switzerland since about 1980 but a connection to the NAO evolution is proposed.

In this article we take as an example two of the devastating wind storms that occurred along the month of January 2018 in Western Europe and analyze, using event attribution techniques, how the frequency of such storms has been and will be altered by human activities. For the first time we analyse both observations and high-resolution regional climate projections for our analysis, which are shown to fairly well simulate extreme wind speeds that are present in such storms.

In Section 2, we describe the meteorological context of the stormy month of 2018 in Western Europe, the events studied and their impacts. In Section 3, a quantitative characterization of the events is provided based on the analysis of observations. In Section 4, models and observations used are described. Sections 5 and 6 develop the analysis of each of the two storms analyzed and Section 7 provides a summary and synthesis of the findings.

## 25  2 The stormy month of January 2018 and the studied storm cases

The year 2018 started with a series of four strong wind storms over Western Europe. In particular, two major events pounded the continent: one on January 3, named Storm Eleanor by the Irish National Meteorological Service, and another one on January 18, named Storm Friederike by the Berlin Institut für Meteorologie.

30   Storm Friederike led to at least eleven casualties and caused major disruptions in the Netherlands and parts of Germany. In advance of Storm Friederike, warnings were issued in both the Netherlands and in Germany for severe wind gusts. On January 17,the timing of the strongest winds was around 9-11 AM, just after the peak of the morning commute, with many people

already on the road and in some cases caught by the strong winds. In addition to the wind hazard, snow created icy road conditions, and people were killed by falling trees or in car accidents caused by dangerous road conditions. In Germany, Storm Friederike is estimated to have caused around €1,6 billion worth of damage, according to the Insurance Journal (2018). They estimate this was the second most expensive storm to strike Germany in the past 20 years. In the Netherlands, three people

5 were killed during the storm. For the first time in history, train traffic was completely shut down across the country. Amsterdam Airport Schiphol was closed and more than 300 flights were canceled. Numerous roads were blocked by fallen trees and overturned trucks. Due to their height, trucks were susceptible to being blown off the roads, which caused disruptions and accidents.

10 The other major storm, Storm Eleanor led to major disruptions in France during the ski holiday season and is estimated to have cost as much as 700M€ (Insurance Journal, 2018). Ski resorts were closed for one or two days in the Alps, with significant economic consequences. Wind gusts of more than 130 km/hr and nearing 150 km/h were reported over several flat regions in France and in Switzerland. Large waves at the Atlantic coasts of Spain and France killed two people. Over France, according to the severity index developed by Météo-France, Eléanor was the sixth most severe storm since 1995.

The strongest wind gusts as estimated from the European Centre for Medium-range Weather Forecast (ECMWF) forecast model are shown in Figure 1 for both storms, which have a very different pattern.

More storms than these two were reported during the month. For instance, Storm Carmen, which preceded Storm Eleanor by

20 two days, crossed Southern France with wind gusts exceeding 130 km/h. On January 17, another storm, Fionn, passed over parts of the Mediterranean region and broke wind speed records, including at Cap Corse at the northern tip of Corsica (225 km/h). From a monthly view and in terms of number of events, January 2018 is the stormiest month since 1998 in France.

The storm activity was due to a strong westerly flow that persisted throughout the month (as shown in Figure 2, first row) and

25 was enhanced by the jet stream extension eastward of its normal position. The persistence of the flow is also characterized by the frequency of occurrence of the so-called "zonal weather regime" (ZO), as defined by Michelangeli et al. (1995) using cluster analysis on Sea Level Pressure (SLP) data from the NCAR/NCEP reanalysis. Approximately 45% of the January days were classified in this cluster (Figure 2, remaining panels), which is characterized by mild and wet winter weather. The average frequency of the ZO weather regime is close to 25%. Although not exceptional, this high frequency is significantly higher than

30 normal.

## 3. Event definitions

Storm Friederike was the result of rapidly developing cyclogenesis and the area with highest wind speeds, located south of the trough center, moved fast from west to east. It crossed the Netherlands and mid-Germany in about half a day. In this analysis,

the salient event characteristics will be represented by an indicator defined on the basis of daily maximum wind speed, derived from observations available from the Integrated Surface Database ("Lite" version, ISD-Lite, Smith et al., 2011). The database contains global hourly weather data for eight variables. Many of these observations are made at airports from cup anemometers. However, many stations only contain three-hourly data for the earlier part of the record. Also, when analyzing model output

5   from some of the models contributing to EURO-CORDEX, the daily maximum near-surface wind speed was obtained on the basis of three-hourly wind speeds. For these reasons, we only sampled observations every three hours and the daily maximum wind speed was calculated only if at least four of the eight sampled observations were available.

In Figure 3, we plot the values of the daily maximum wind observed over Northwestern Europe on the days of the storms. The

10   track of Storm Friederike can be seen in the box [2-15E; 50-53N] where wind speeds are largest. We, therefore, selected as the event indicator the seasonal (December-January-February, DJF) maximum value of this land area average of daily maximum wind speed (see also Figure 2).

This area contains 68 stations observing wind speed. The area average cannot be exactly calculated using the stations because

15   the distribution of the stations is not even or dense enough, but we take the station average as a reasonable approximation. Using this indicator, Storm Friederike is the eleventh strongest storm in the area since 1 January 1976, with an indicator value of 16.0 ms$^{-1}$ max daily wind. The 2017-2018 winter season (DJF) becomes the seventh in terms of strongest winter winds over this station set. However this storm was not the 7th strongest storm as some seasons had multiple stronger storms. We also considered the daily mean wind for models that did not store higher-frequency data. In terms of that indicator, Friederike was

20   not remarkable with 8.7 m/s$^{-1}$, as it was a very short duration storm with a calm period immediately following it, bringing the daily mean to a moderate value.

For models, the area average is calculated over land grid points, which slightly lowers the indicator value (see comparisons in Table 1 for model evaluation) as the stations are concentrated near the coast where the intensity was higher. In order to calculate

25   seasonal return periods, we take the maximum value of the indicator over the winter season (DJF).

The structure of Storm Eleanor was very different. Eleanor was embedded in a deep large-scale low pressure system. Its strong winds affected a much broader area than Storm Friederike: from Ireland and the U.K. via western France, to Switzerland and the Riviera coast. Its high wind speeds, unusual in Western Europe constituted its most striking aspect. As this storm, also,

30   passed within a day we construct  the same indicators as for Friederike, which are daily maximum and mean of wind speed, but averaged over a much wider area, from 0 to 10°E and 42°N to 52°N (see Figure 1b and 3b). The value of the indicator is 12.3 m/s for maximum winds and 8.3 m/s for daily mean winds.

## 4. Observations, model ensembles and evaluation

For the observational part of the attribution analysis, we used two sources of station data. Unfortunately, the available quantities were slightly different in the different datasets. The analysis is mainly based on the ISD-lite database described above, in which we used the daily maximum of three-hourly instantaneous wind speed. Additional results are based on the KNMI

5  climatological service database, which provides the daily maximum of the hourly averaged wind speed. The highest hourly wind of the year series were visually quality controlled. For three series, early data was discarded for obvious inhomogeneities supported by the metadata (Leeuwarden <1990, De Bilt <2002, Lichteiland Goeree <1995). Most series start in 1981, but they are notably more variable and possibly unreliable before circa 1990.

10  The KNMI data have also been converted to potential winds, i.e., the wind speed at 10 m that would have occurred assuming a roughness length of 3 cm over land and 2 mm over water, and assuming neutral stability (Wever and Groen, 2009). Such calculation is made by multiplying wind speeds by "exposure correction factors" which to first order account for changes in the elevation of the wind anemometer and changes in roughness surrounding the station in different directions. These factors are deduced from the high-frequency variability of the wind (intra 10 min standard deviation or wind gust). These exposure

15  correction factors are recomputed every 3 years. Three years of measurements are required to ensure that there are at least 10 appropriate measurements in each of the wind direction sectors. If a new exposure correction factor is found to be significantly different (absolute difference > 0.05) from the existing factor the new factor is introduced.

We used four climate model simulation ensembles. The first ensemble is the RACMO regional climate model ensemble

20  downscaling 16 initial-condition realizations of the EC-EARTH 2.3 coupled climate model in the CMIP5 RCP8.5 scenario (Lenderink et al., 2014, Aalbers et al., 2017). The RACMO model uses a 0.11° (12 km) resolution and the daily maximum of near-surface wind speed is analyzed. In RACMO, the near-surface wind speed is diagnosed from the model wind and stability vertical profile as the wind speed at 10 m, applying a roughness length of at most 3 cm for land grid points, and a Charnock-type relation for sea grid points. This ensemble was previously used to estimate the change in the odds of wind stagnations in

25  Northwestern Europe (Vautard et al., 2017) and was found to simulate monthly wintertime wind speeds over Western Europe in a satisfactory manner. RACMO simulations are available for the 1950-2100 period. As in previous analyses (see e.g., Philip et al., 2018),  we use a 20th century early 30-year period [1951-1980] to estimate odds in the past climate, and the 2001-2030 period to estimate odds in the current climate. We also use two future periods, a period called "near future" [2021-2050] and a period called "mid century" [1941-1970]. We only used the simulations using the RCP8.5 radiative forcing scenario. As a

30  cross-check we fitted a time-dependent generalized extreme value (GEV) function to the whole period 1971-2070, as described in van der Wiel et al (2017).

The second model ensemble is the HadGEM3A ensemble (Christidis et al., 2013; Vautard et al., 2018), which includes a set of 15 realizations of atmospheric simulations using observed SSTs (reflecting the actual world) and a set using SSTs where the CMIP5 mean patterns of anthropogenic heat contribution are removed to estimate the ocean response to a pre-industrial atmospheric composition (as the natural/counterfactual world). The latter runs also use pre-industrial greenhouse gas and

5    aerosol concentrations. Land use and, hence, roughness is put to 1850 values in the HistoricalNat ensemble. For this model, the wind speed daily maximum was not available and the daily mean wind was used instead. No future simulations were available.

The third ensemble is the multi-model EURO-CORDEX ensemble (Jacob et al., 2014), using a 0.11° resolution over Europe.

10   For this ensemble, only 11 simulations were used and bias correction was applied (Bartok et al., 2018, in preparation) using the Cumulative Distribution Function transform (CDFt, Vrac et al., 2016). These simulations have been evaluated in the context      of      the      CLIM4ENERGY      Copernicus      Climate      Change      Service      project (http://clim4energy.climate.copernicus.eu). The reference data used for bias correction is the Watch Forcing Data ERA-Interim (WFDEI, Weedon et al., 2014). For wind speed, it is essentially an interpolation of ERA-Interim over a 0.5°×0.5°

15   grid. This data set has a relatively low resolution, so extreme winds are not expected to be accurately represented. This weakness is, therefore, probably propagated to the EURO-CORDEX ensemble. The ensemble is pooled, which is formally possible because the bias correction method corrects data making it homogeneous across the multi-model distribution.

The fourth ensemble is obtained from simulations using the distributed computing framework known as weather@home

20   (Massey et al. 2015). We used four different large ensembles of December-February wind speeds using the Met Office Hadley Centre for Climate Science and Services regional climate model HadRM3P at 25km resolution over Europe embedded in the atmosphere-only global circulation model HadAM3P at N96 resolution. The first set of ensembles represents possible winter weather under current climate conditions. This ensemble is called the "all forcings" scenario and includes human-caused climate change. The second set of ensembles represents possible winter weather in a world as it might have been without

25   anthropogenic climate drivers, using different estimates of pre-industrial SST deduced from the CMIP5 ensemble and pre-industrial greenhouse gas and aerosol concentrations. Land-use in both ensembles is identical. This ensemble is called the "natural" or "counterfactual" scenario (Schaller et al., 2016). The third set of ensembles represents a future scenario in which the global mean surface temperature is 1.5°C higher than pre-industrial global temperatures. The fourth scenario is the same as the third, but for 2°C of future global mean temperature. To simulate the third and fourth scenario, we use atmospheric

30   forcings derived from RCP2.6 and 4.5 and sea surface temperatures that match the atmospheric forcing obtained from CMIP5 simulations (Mitchell et al., 2017).

The evaluation of the models' ability to simulate the indicator is made using the ISD-Lite observations, which are available in near-real time. In order to evaluate the capacity of the models to simulate the winds, we extracted wind speed daily maxima at

the locations of ISD-Lite stations and averaged these values over all stations in the area. Then, we compared the simulated mean, 95th centile and 99th centile, with the observed equivalent for each model ensemble. For HadGEM3-A and weather@home, as daily maxima were not available, we used daily averages of the wind speeds.

5    For RACMO, HadGEM3-A and weather@home, model values are pooled together to compute the distribution statistics. For EURO-CORDEX, we calculated both individual model and pooled statistics. Results are presented in Table 1 for the average over all grid points closest to the 68 ISD-lite stations, together with equivalent statistics when the average is made over all land grid points, instead of the positions of the stations. Results show that the models reproduce the indicator with success along the distribution. Comparisons to station data indicate a general underestimation of models within a 10% range. EURO-
10   CORDEX simulations are bias corrected, so the bias is essentially reflecting the WFDEI (ERA-Interim based) bias. The fact that statistics do not differ from one model to the other supports pooling the models' simulations together in a common distribution. This bias is consistent with models not simulating observational noise due to remaining turbulence. For weather@home, we only have daily values for mean wind speed, so we calculate the maximum mean area-averaged daily wind speed in a winter season. The simulated values are higher than the observed values for this quantity, especially for the
15   mean, while the 95th and 99th quantile are comparable to observations in particular for the Storm Friederike.

Grid point averages reach lower values than station averages, which is a probable consequence of the higher density of stations near the North Sea coast where winds are stronger, which is reflected in the observed area average. The factor between observation statistics and model statistics for station averages is rather uniform across the distributions, even though
20   observations seem to be heavier tailed than simulations. In order to homogenize attribution results among models and observations and compare return periods with observations, we scaled all simulations by the ratio between 99th centiles of observed station averages and simulated grid-point averages. These bias corrections are a factor 1.13 for RACMO (for both storms), 1.17 (resp. 1.28) for EURO-CORDEX for Friederike (resp. Eleanor), and 1.12 (resp. 1.22) for HadGEM3-A for Friederike (resp. Eleanor).

## 5. Storm Friederike

### 5.1 Observations

The winter maximum of the daily maximum of three-hourly maximum wind over the ISD-lite spatial average (over all stations in the box) is shown in Fig. 4a as a function of time (labeled with the year of the second half of winter). The data has been
30   fitted by a GEV distribution in which the location parameter $\mu$ and scale parameter $\sigma$ vary exponentially with time, such that their ratio remains constant. The shape parameter $\xi$ is not time-dependent. (We checked whether these assumptions are valid in the models that have enough data not to need these assumptions.) This fit shows a significant decrease ($p<0.05$ two-sided)

in wind speed over 1976–2017, in agreement with earlier analyses (Smits et al, 2005, Vautard et al, 2010). The decrease in intensity of about 12% (95% CI 0–30%) corresponds to a decrease in probability of about a factor of four (95% CI: 1 to 100). Using the global mean temperature as a covariate instead of time gives slightly higher trends. The shape parameter $\xi$ of the GEV is most likely negative, so the distribution has a tail that is thinner than an exponential distribution. This implies that the

5 ratio of probabilities is larger for the same difference in wind speed for a higher baseline, i.e., stronger storms.

The return period of an event like Friederike or worse in the area in which the indicator value reached 16.0 m/s on January 18 in the current climate is of the order of 20 years. In the 1970s, this was roughly five years, so the event, defined using our indicator, has become a fairly rare event due to the decrease in high wind speeds observed during this period.

The result is confirmed in a different dataset from KNMI observations, with most stations showing a clear downward trend over the whole period (1971–2017 for two stations, 1982–2017 for most others, at least 30 years with data). A simultaneous fit to all stations scaled to the same mean show a decrease in intensity of −15% [−7% to −17%], the same as the ISD-lite data show. The trends are much less clear when starting in 1990 (using stations with at least 25 years of data). The trends in potential

15 wind are much smaller (around −5%) and not statistically significant from zero, even when pooled over all stations.

## 5.2 RACMO ensemble

The storm indicator is scaled to have the same 99th centile as the observed indicator in the historical period. Indicator statistics are then obtained for three climate periods: 1951-1980, simulating the "past" period, the "current" period taken as 2001-2030,

20 and two future periods assuming the RCP8.5 scenario (2021-2050 and 2041-2060). The observed indicator value for storm Friederike (16.0 m/s) has a present return period of about 13 years (95% CI 10-19 years), which is longer than for the observations. The probability of witnessing higher indicator values is not significantly different in past and current periods (Figure 5). However, the change of probability becomes larger in future periods, with a probability ratio (PR) of about 1.5 [1-2] in the near term (Figure 5b). For this particular case, the increase is also stronger for stronger storms due to an increase in

25 the variability relative to the mean.

Therefore, according to this model's representation, we do not identify a climate change impact currently, but the increase in probability of storms like Friederike emerges in the coming decades. A fit with a GEV that scales with the global mean temperature of the driving EC-Earth ensemble gives no change (PR between 0.95 and 1.16), overlapping with the 30-year time

30 window analysis (not shown), but this does not include the increase of variability relative to the mean.

### 5.3 HadGEM3A ensemble

The HadGEM3-A ensemble exhibits a significant difference between actual and counterfactual periods, with a current increase of strong daily mean winds in the area struck by Storm Friederike. However, due to the use of the mean wind speed instead of the maximum wind speed, the indicator does not disentangle extreme winds over a short time period from less strong winds
5    over an extended time period. Accordingly, the observed value is not exceptional, due to the fast travelling nature of the extremely high winds in the area: for the value corresponding to Friederike (8.7 m/s), such events occur almost every year in both types of simulations.

### 5.4 EURO-CORDEX ensemble

10   In the EURO-CORDEX simulations, the return period corresponding to the scaled indicator (25-40 years) is larger, making it a more extreme event. The shape of the distribution is clearly different from that of the RACMO simulations and that of the observations (compare with Figs. 4 and 5). The PR is generally not significantly different from one (Figure 7b), despite a rather systematic increase. Such increase becomes marginally significant in the middle of the century with PR values in the range 1 to 3 for lower wind thresholds. Again, this indicates a tendency for more storms like Friederike in the future with a signal
15   emergence not yet achieved. The GEV with smoothed EC-Earth global mean temperature as covariate confirms this conclusion, with an increase in probability of 1.0 to 1.2 ($p\sim0.1$), this corresponds to the assumption the percentage increase is a constant 0.0 to 1.4% per degree global warming over the whole range of Fig. 7a. This assumption holds well over the four 30-year time periods considered before.

### 5.5 Weather@Home

For weather@home, using the suboptimal definition of maximum of daily mean wind to define Storm Friederike (8.7 m/s), we find no significant change in the likelihood of storms like Friederike to occur (Figure 8). In contrast to the EURO-CORDEX assessment this also holds for rarer events (not shown).

## 6. Storm Eleanor

### 6.1 Observations

The same observational analysis on the Eleanor index as in section 4.1 gives a more significant downward trend for this storm ($p<0.01$ two-sided), with a decrease of about 20% (3–35%) (Figure 9). This corresponds to an increase in return period of a
30   factor 8 (1.5–100). The return time also is about 20 years in the current climate according to this fit.

## 6.2 RACMO ensemble

Storm Eleanor is now investigated through the wind daily maximum indicator with an average over the large region as defined above. Due to the southern boundary that is excluding a small band of the large region, we used for this model a boundary at 43.5N instead of 42N. This makes the indicator return value for stations slightly lower than when calculated over the full region (11.9 m/s instead of 12.3 m/s). The corresponding RACMO return period is in the range 3 to 5 years. The climate change is not significant for the current period and marginally significant for future periods, as for Storm Friederike (Figure 10). The estimated PR is 1.1 and slightly higher for future periods. Interestingly, for stronger storms, the PR increases. The same results hold for a GEV fit with covariate of all data in 1971-2070, with a PR significantly different from one (95% CI 1.0 to 1.2, not shown).

## 6.3 HadGEM3A ensemble

For HadGEM3-A, using the daily mean wind, we find no climate change signal in the estimation of the probabilities of high winds of any magnitude, but for the very extreme winds, we find marginally significant changes in the direction of more frequent high winds under current conditions than under natural conditions (Figure 11). The estimated return period for the indicator value corresponding to Eleanor, which does not fall in the extreme tail, lies also between three and five years.

## 6.4 EURO-CORDEX ensemble

Using the EURO-CORDEX ensemble, the return period of the large-scale Storm Eleanor, characterized by the chosen indicator, is estimated to about 7-10 years. A climate change signal is absent in the simulations when comparing 1971-2000 and 2001-2030 periods. For the indicator value, the PR is in the range [0.5-1]. Only for later periods and for larger indicator values, a marginally significant increase in the PR in the range [1-2] can be seen (Figure 12). A GEV with a modelled global mean temperature (from EC-Earth) as covariate also gives a non-significant increase with a PR between 0.99 and 1.15 (95% CI).

## 6.5 Weather@Home

For weather@home, using the maximum of daily mean wind to define Storm Eleanor (8.3 m/s), we find no significant change in the likelihood of storms like Eleanor to occur. In contrast to the EURO-CORDEX assessment, this also holds for rarer events where the weather@home model shows a non-significant decrease in high wind speeds.

**6. Synthesis and conclusions**

5   Western European countries have been struck by high-impact wind storms during the month of January 2018. The link between storms like Eleanor (on 3/1/2018) and Friederike (on 18/1/2018) and human-induced climate change have been studied through this attribution analysis involving several simulation ensembles and observations from tens of weather stations.

From an analysis of two sets of observations, we conclude that near-surface storms in the areas of the two storms have a
10   decreasing trend in wind speed and, hence, in frequency over the past 40 years (see Figure 13), consistent with previous observation-based studies on storminess in these areas (Smits et al., 2005; Soubeyroux et al., 2017) and with global land wind stilling (Vautard et al., 2010; McVicar et al., 2012). This trend was shown to be close to zero over the Netherlands area when using the potential wind, indicating a strong influence of roughness changes there, as also demonstrated by Wever, 2012. Other processes, such as aerosols increase, could also induce a wind decrease (Bichet et al., 2012), and decadal-scale long-term
15   variability has been shown to have a significant role as well (e.g., Matulla et al, 2008).

We next turn to the model results. Due to the differing experiments that we used, the probability ratios have been computed over different intervals. To compare those we need to convert them to a common interval. We do this by assuming the probability ratio is an exponential function of some indicator of global warming $f(\text{yr})$:

$$PR(y_1, y_{end}) = PR(y_2, yr_{end}) \, PR(yr_1, yr_2) = PR(yr_2, yr_{end}) \exp[f(yr_1) - f(yr_2)]$$

In the following, we use the RCP4.5 $CO_2$ concentration for $f(\text{yr})$, as the global mean temperature has no observations in the future and the projections depend on the model.

In contrast to the observations, global and regional climate models do not simulate such a decrease over the past decades. Instead, simulations of the daily maximum of 3-hourly instantaneous wind, of the same spatial and temporal characteristics of these storms and, hence, the observational analysis, indicate increases in probability between 1975 and 2055, corresponding to increases in wind speed for this return time (figure 14). These are not all significantly different from one, but model
30   consensus and future trends support the presence of such positive tendency. The change is small though: a probability ratio of 1.5 for Friederike with an uncertainty range of 1 to 2, corresponding with an increase in intensity of the wind of only about

5% (0% to 10%). For Eleanor, the numbers are even smaller: an increase in PR of about 1.25 (1.0 to 1.6) or an increase in intensity of 2% (0% to 5%).

The changes in daily mean wind are smaller still and indistinguishable from no change. However, as these do not correspond
5   directly to the impact of these storms, we do not take them into account in the synthesis.

The climate model simulations do not always include changes in aerosols and either have no roughness changes (regional models) or capture these only partially (HadGEM3-A). This explains at least partially the conflict with the observed trends, as the potential wind results for the Netherlands showed that roughness plays a large role in the observed decrease in storminess.
10  By contrast, these model ensembles mainly reflect changes due to greenhouse gases.

We conclude that storms like Friederike and Eleanor have not become significantly more or less frequent due to climate change, but our model results indicate that global warming due to greenhouse gases could make storms like them somewhat more frequent in the future, with a frequency increase up to at most a factor of two, or equivalently a few percent higher wind speeds.
15  However, this may seem contradictory with the observations showing a clear and significant decline in high wind speeds, in accordance with earlier studies. This is equivalent to declining probabilities of these kind of storms, but our analysis and previous studies find explanations for these changes in factors other than greenhouse gases. The increase in roughness potentially explains a major part of this decrease (Vautard et al., 2011; Wever et al, 2012), and does not exclude other factors, such as decadal variability and aerosol effects. Until a quantitative attribution of past observed decreases is established, and
20  with that an understanding of the interplay between greenhouse gas forcing and those other factors, and scenarios for them, the confidence on future evolutions of wind storms will remain low, based on simulations reflecting mainly the effects of greenhouse gas increases.

**Acknowledgements**

This work was supported by the EUPHEME project, which is part of ERA4CS, an ERA-NET initiated by JPI Climate and co-
25  funded by the European Union (Grant #690462). It was also supported by the French Ministry for an Ecological and Solidary Transition through national convention on climate services. We would like to thank all volunteers who have donated their computing time to weather@home. The work was initially published by the same authors on the World Weather Attribution web site: https://www.worldweatherattribution.org/, as a "rapid attribution study", and this article is taking most of the material from this analysis and refined it.

30

# References

Aalbers, E.E., G. Lenderink, E. van Meijgaard, and van den Hurk, B.J.J.M.: Local-scale changes in mean and heavy precipitation in Western Europe: climate change or internal variability? *Clim. Dyn.* doi: 10.1007/s00382-017-3901-9, 2017.

5 Barredo, J. I.: No upward trend in normalised windstorm losses in Europe: 1970–2008, Nat. Hazards Earth Syst. Sci., 10, 97-104, https://doi.org/10.5194/nhess-10-97-2010, 2010.

Bengtsson, L., Hodges, K. I., and Roeckner, E. Storm tracks and climate change. Journal of Climate, 19(15), 3518-43, 2006.

10 Beniston, M.: Current and Future Trends of Climatic Extremes in Switzerland. Geography Compass, 1: 739-751. doi:10.1111/j.1749-8198.2007.00043.x, 2007.

Bichet, A., Wild, M., Folini, D., and Schär, C.: Causes for decadal variations of wind speed over land: Sensitivity studies with a global climate model. *Geophysical Research Letters*, *39*(11), 2012.

Christidis, N., Stott, P. A., Scaife, A. A., Arribas, A., Jones, G. S., Copsey, D., Knight, J. R. and Tennant, W. J.: A new HadGEM3-A-based system for attribution of weather-and climate-related extreme events. *Journal of Climate*, *26*(9), 2756-2783, 2013.

20 Haarsma, R. J., Selten, F., and van Oldenborgh, G. J.: Anthropogenic changes of the thermal and zonal flow structure over Western Europe and Eastern North Atlantic in CMIP3 and CMIP5 models. *Climate Dynamics*, 41(9-10), 2577-2588, 2013.

Insurance Journal, 2018, https://www.insurancejournal.com/news/international/2018/04/17/486633.htm

25 Lenderink, G., van den Hurk, B. J. J. M., Klein Tank, A., van Oldenborgh, G. J., van Meijgaard, E., de Vries, H., and Beersma, J. J.: Preparing local climate change scenarios for the Netherlands using resampling of climate model output. Environ. Res. Lett., 9, 11, 115008, doi:10.1088/1748-9326/9/11/115008, 2014.

Martínez-Alvarado, O., Gray, S. L., Hart, N. C., Clark, P. A., Hodges, K., and Roberts, M. J.: Increased wind risk from sting-30 jet windstorms with climate change. Environmental Research Letters, 13(4), 044002, 2018.

Massey, N., Jones, R., Otto, F. E. L., Aina, T., Wilson, S., Murphy, J. M., Yamasaki, Y. H., and Allen, M. R.: weather@ home—development and validation of a very large ensemble modelling system for probabilistic event attribution. Quarterly Journal of the Royal Meteorological Society, 141(690), 1528-1545, 2015.

5    Matulla, C., Schöner, W., Alexandersson, H., and von Storch, H.: European storminess: late nineteenth century to present, Clim. Dyn., 31, 125–130, doi:10.1007/s00382-007-0333-y, 2008.

McVicar, T. R., Roderick, M. L., Donohue, R. J., Li, L. T., Van Niel, T. G., Thomas, A., Grieser, J., Jhajharia, D., Himri, Y., Mahowald, N. M., Mescherskaya, A. V., Kruger, A. C., Rehman, S., and Dinpashoh, Y.: Global review and synthesis of trends
10   in observed terrestrial near-surface wind speeds: Implications for evaporation. *Journal of Hydrology*, *416*, 182-205, 2012.

Michelangeli, P.A., Vautard, R., and Legras, B.: Weather regimes: recurrence and quasi-stationarity, *J. Atmos. Sci.*, 52, 1237-1256, 1995.

15   Mitchell, D., AchutaRao, K., Allen, M., Bethke, I., Beyerle, U., Ciavarella, A., Forster, P. M., Fuglestvedt, J., Gillett, N., Haustein, K., Ingram, W., Iversen, T., Kharin, V., Klingaman, N., Massey, N., Fischer, E., Schleussner, C.-F., Scinocca, J., Seland, Ø., Shiogama, H., Shuckburgh, E., Sparrow, S., Stone, D., Uhe, P., Wallom, D., Wehner, M., and Zaaboul, R.: Half a degree additional warming, prognosis and projected impacts (HAPPI): background and experimental design. Geoscientific Model Development, 10(2), 571-583, 2017.

Nissen, K. M., Leckebusch, G. C., Pinto, J. G., and Ulbrich, U.: Mediterranean cyclones and windstorms in a changing climate. Regional environmental change, 14(5), 1873-1890, 2014.

Philip, S., Kew, S. F., van Oldenborgh, G.-J., Aalbers, E., Vautard, R. Otto, F. E. L., Haustein, K., Habets, F., Singh, R. and
25   Cullen, H.: Validation of a rapid attribution of the May/June 2016 flood-inducing precipitation in France to climate change, Climate Dynamics, submitted, 2018.

Schaller, N., Kay, A. L., Lamb, R. Massey, N. R., van Oldenborgh, G.-J., Otto, F. E. L., Sparrow, S. N., Vautard, R., Yiou, P., Bowery, A., Crooks, S. M., Huntingford, C., Ingram, W., Jones, R., Legg, T., Miller, J., Skeggs, J., Wallom, D., Wilson, S.
30   and Allen, M. R.: Human influence on climate in the 2014 Southern England winter floods and their impacts. Nature climate change, doi:10.1038/nclimate2927, 2016.

Smith, A., N. Lott, and Vose, R.: The integrated surface database: Recent developments and partnerships. Bull. Amer. Meteor. Soc., 92, 704-708, doi:10.1175/2011BAMS3015.1, 2011.

Smits, A. A. K. T., Klein Tank, A. M. G., and Können, G. P.: Trends in storminess over the Netherlands, 1962–2002. *International Journal of Climatology*, *25*(10), 1331-1344, 2005.

5  Soubeyroux, J.-M., Dosnon, F., Richon, J., Schneider, M., and P. Lassègues: Caractérisation à haute résolution spatiale des tempêtes historiques en métropole application à la tempête Zeus du 6 mars 2017. La Climatologie, 14, 2017.

Ulbrich, U., Pinto, J. G., Kupfer, H., Leckebusch, G. C., Spangehl, T., and Reyers, M.: Changing Northern Hemisphere storm tracks in an ensemble of IPCC climate change simulations. Journal of climate, 21(8), 1669-1679, 2008.

Ulbrich, U., Leckebusch, G. C., and Pinto, J. G.: Extra-tropical cyclones in the present and future climate: a review. Theoretical and Applied Climatology, 96(1-2), 117-131, 2009.

van der Wiel, K., Kapnick, S. B., van Oldenborgh, G. J., Whan, K., Philip, S. Y., Vecchi, G. A., Singh, R. K., Arrighi, J. and
15  Cullen, H.: Rapid attribution of the August 2016 flood-inducing extreme precipitation in south Louisiana to climate change. Hydrol. Earth Syst. Sci., 21, 897–921, 2017.

Vautard, R., Cattiaux, J., Yiou, P., Thepaut, J.-N., and Ciais, P.: Northern Hemisphere atmospheric stilling partly attributed to an increase in surface roughness. Nature Geoscience, 3, 756–761, 2010.

Vautard, R., Colette, A., van Meijgaard, E., Meleux, F., van Oldenborgh, G. J., Otto, F. E. L., Tobin, I., and Yiou, P.: Attribution of wintertime anticyclonic stagnation contributing to air pollution in Western Europe. *Bull. Am. Meteor. Soc.*, in "Explaining extreme events of 2016 from a climate perspective", special supplement, S70-S75, 2017.

25  Vautard, R., Gobiet, A., Sobolowski, S., Kjellström, E., Stegehuis, A., Watkiss, P., Mendlik, T., Landgren, O., Nikulin, G., Teichmann, C., and Jacob, D.:, The European climate under a 2°C global warming. Environ. Res. Lett., doi:10.1088/1748-9326/9/3/034006, 2014.

Vautard, R., Christidis, N., Ciavarella, A., Alvarez-Castro, C., Bellprat, O., Christiansen, B., Colfescu, I., Cowan, T., Doblas-
30  Reyes, F., Eden, J., Hauser, M., Hegerl, G., Hempelmann, N., Klehmet, K., Lott, F., Nangini, C., Orth, R., Radanovics, S., Seneviratne, S. I., van Oldenborgh, G. J., Stott, S., Tett, S., Wilcox, L., and Yiou, P.: Evaluation of the HadGEM3-A simulations in view of climate and weather event human influence attribution in Europe. Climate Dynamics, doi:10.1007/s00382-018-4183-6, 2018.

Vose, R.S., Applequist, S., Bourassa, M. A., Pryor, S. C., Barthelmie, R. J., Blanton, B., Bromirski, P. D., Brooks, H. E., DeGaetano, A. T., Dole, Easterling, R. M., Jensen, R. E., Karl, T. R., Katz, R. W., Klink, K., Kruk, M. C., Kunkel, K. E., MacCracken, M. C., Peterson, T. C., Shein, K., Thomas, B. R., Walsh, J. E., Wang, X. L., Wehner, M. F., Wuebbles, D. J., and Young, R. S.: Monitoring and Understanding Changes in Extremes: Extratropical Storms, Winds, and Waves. Bull. Amer.

5   Meteor. Soc., 95, 377–386, https://doi.org/10.1175/BAMS-D-12-00162.1, 2014.

Vrac, M., Noël, T. and Vautard, R.: Bias correction of precipitation through Singularity Stochastic Removal: Because occurrences matter, J. Geophys. Res., *121*(10), 5237-5258, 2016.

10   Weedon, G. P., Balsamo, G., Bellouin, N., Gomes, S., Best, M. J., and Viterbo, P.: The WFDEI meteorological forcing data set: WATCH Forcing Data methodology applied to ERA-Interim reanalysis data. Water Resources Research, 50(9), 7505-7514, 2014.

Wever, N. and Groen, G.: Improving potential wind for extreme wind statistics, KNMI Scientific Report WR 2009-02, 2009.

Wever, N.: Quantifying trends in surface roughness and the effect on surface wind speed observations. *Journal of Geophysical Research: Atmospheres*, *117*(D11), 2012.

Yin, J. H.: A consistent poleward shift of the storm tracks in simulations of 21st century climate. Geophysical Research Letters,

20   32(18), 2005.
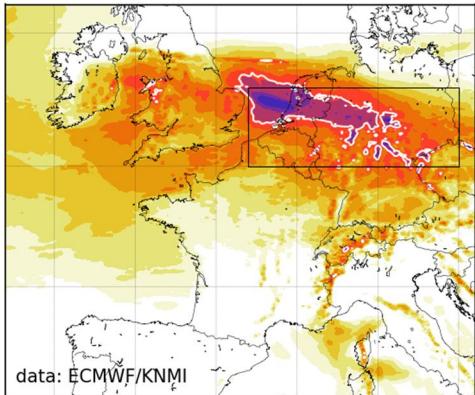
# Figures
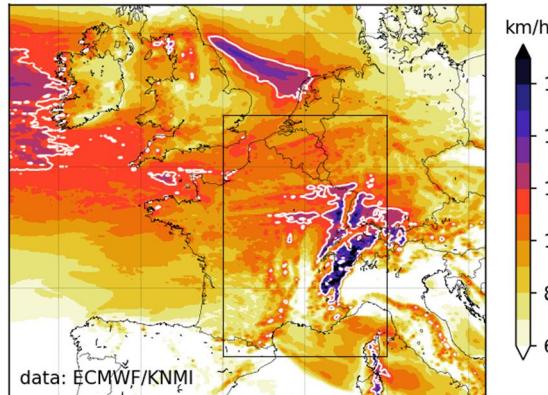
a) Storm Friederike                    b) Storm Eleanor

**Figure 1: Strongest wind gusts during the storms Friederike (a) and Eleanor (b) as estimated from the ECMWF deterministic forecasts starting at 2018-01-18 00UTC and 2018-01-03 00UTC respectively. White contours are used to indicate areas where gusts exceed 118 km/hr. The boxes indicate the spatial event definitions (section 2).**
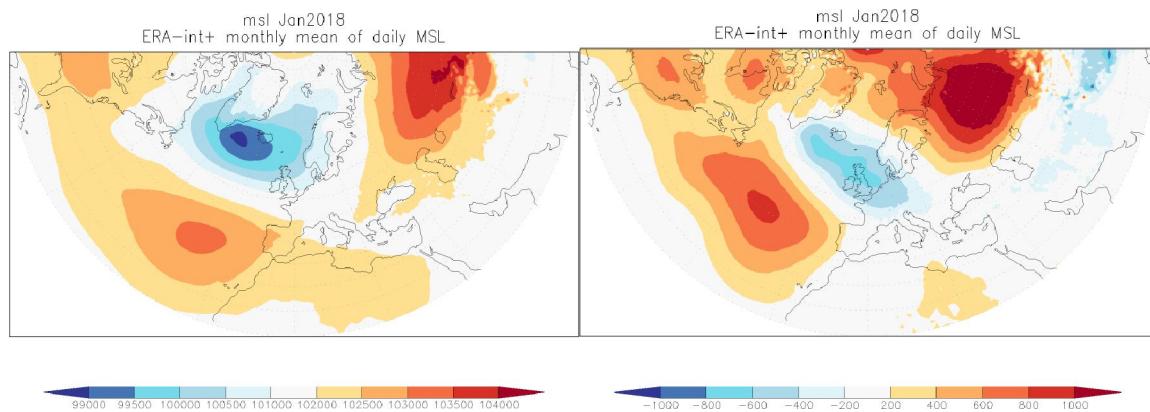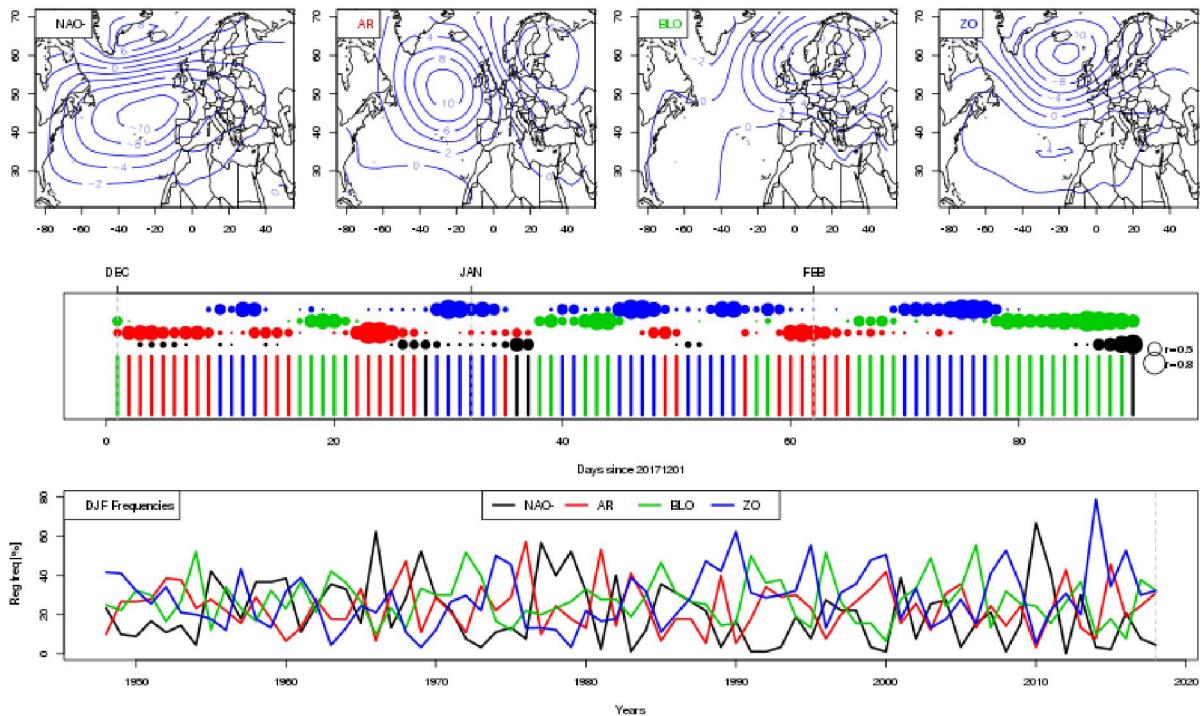
**Figure 2: Top row: Sea level pressure (left) and anomaly (right) (ECMWF analysis, ERA-Interim climatology); b) second row: Weather regime cluster centroids from NCAR/NCEP reanalysis; middle: occurrence of weather regimes from 1st December 2017 to 28th February 2018; the vertical bars indicate the preferred centroid (NAO-, Atlantic Ridge, Scandinavian Blocking, Zonal) and the colored circles indicate the spatial correlation with the prefered centroid; bottom: weather regime wintertime frequencies from 1948 to 2018.**
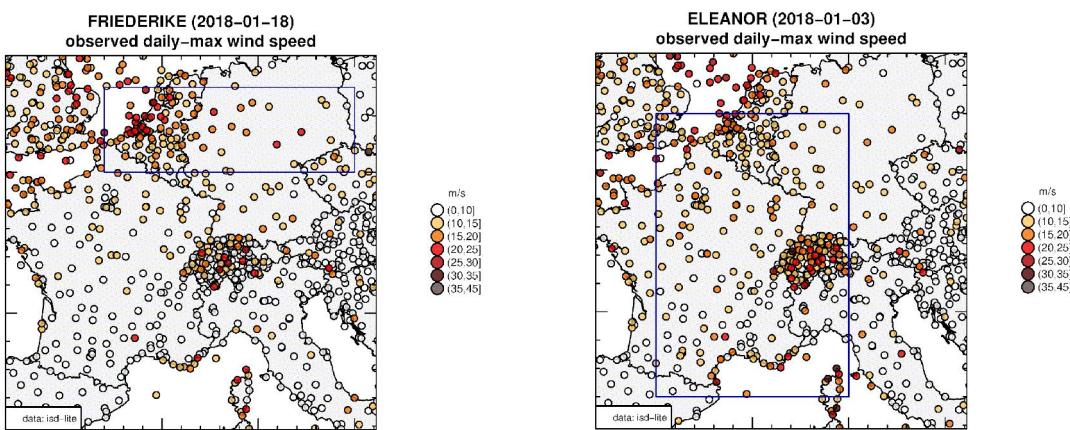
a.     *Storm Friederike*                              *b) Storm Eleanor*

**Figure 3: a) Daily maximum wind speeds at ISD-Lite stations over Northwestern Europe and area defining the event indicator**
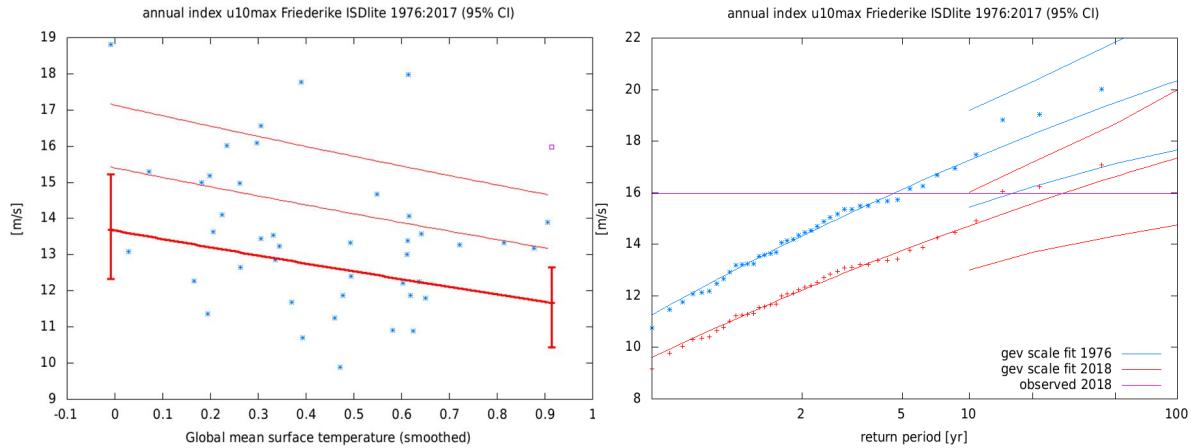
5  **Figure 4. a) Highest winter value of the Friederike index described in Section 2 fitted to a GEV function that scales with time. The thick line denotes the position parameter μ, the thin lines μ+σ and μ+2σ. b) The GEV fit as a function of return period for the climate of 1976 (blue, observations have been scaled up with the fitted trend) and 2018 (red).**
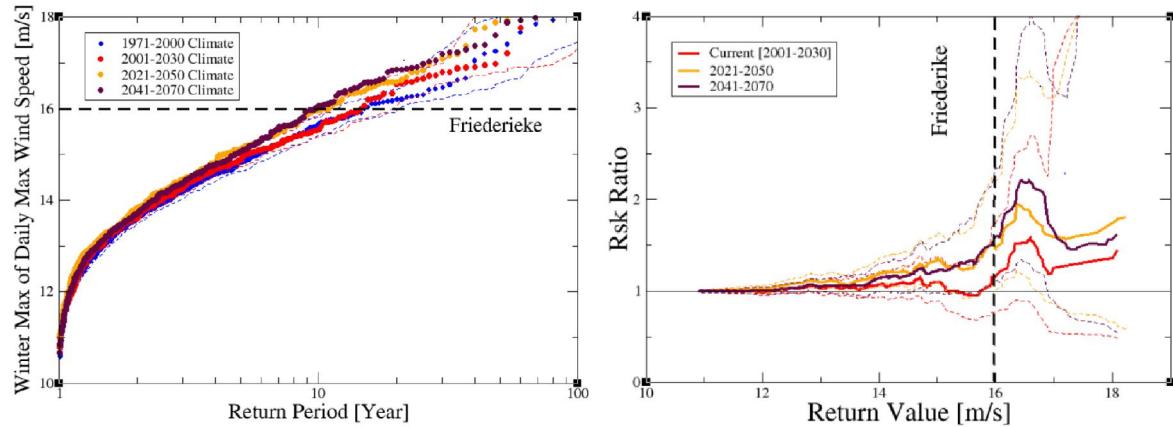
**Figure 5: (left) Return values as a function of return periods for the Storm Friederike indicator, for different time periods and the**
10 **RACMO ensemble; (right) Probability ratio of exceeding the return value of the indicator as compared with counterfactual period as a function of the return value, with 5-95% significance intervals, calculated from a nonparametric bootstrap.**
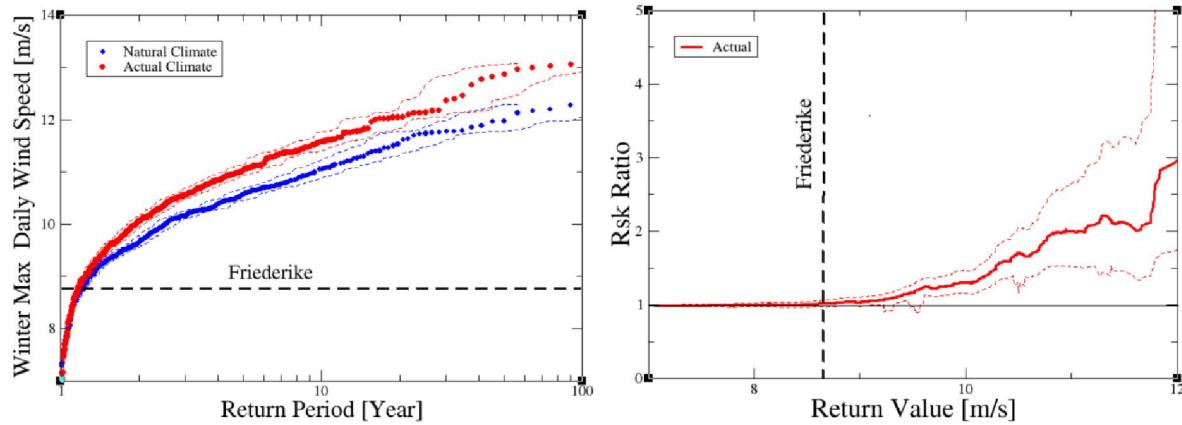
**Figure 6: (left) Return values as a function of return periods for the Storm Friederike indicator, for the HadGEM3-A ensemble; (right) Probability ratio of exceeding the return value of the indicator as compared with counterfactual period as a function of the return value, with 5-95% significance intervals, calculated with a nonparametric bootstrap.**
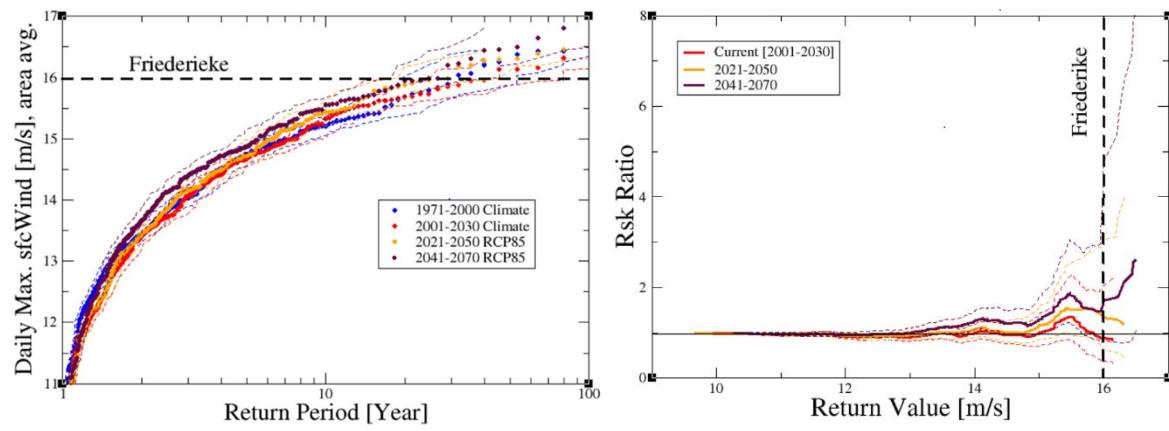
**Figure 7: Same as Figure 5 but for the EURO-CORDEX ensemble**
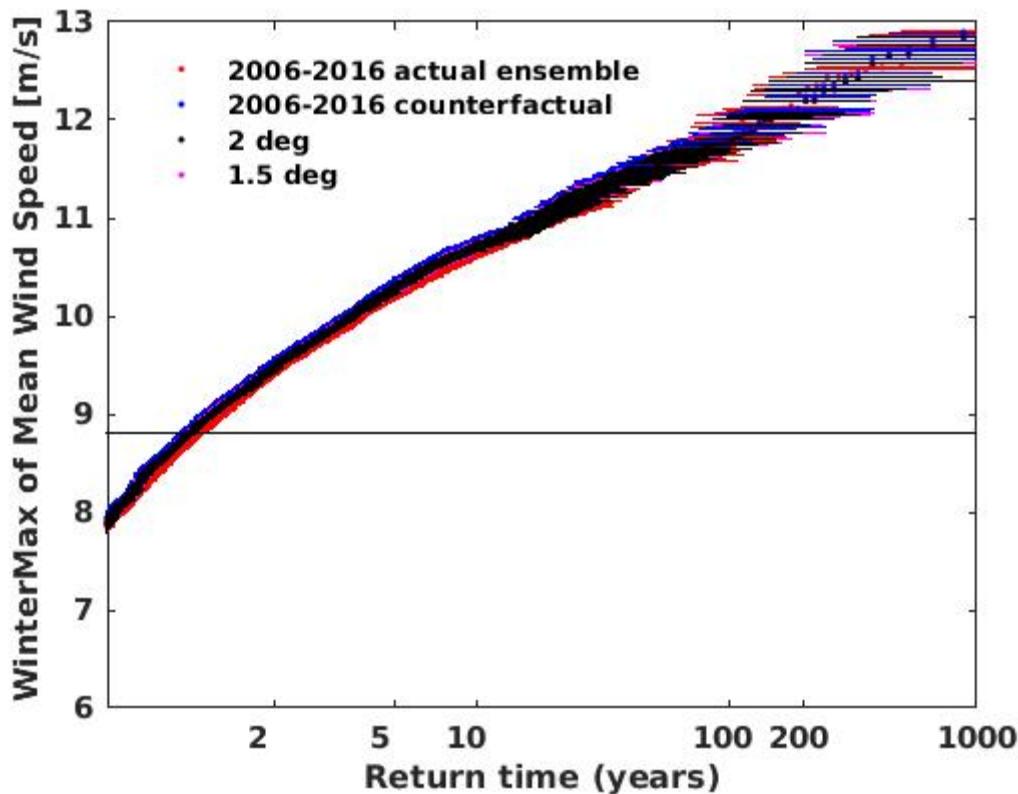
**Figure 8: Return values as a function of return periods for the Storm Friederike indicator, for the weather@home ensemble with 5-95% significance intervals, calculated from a nonparametric bootstrap.**
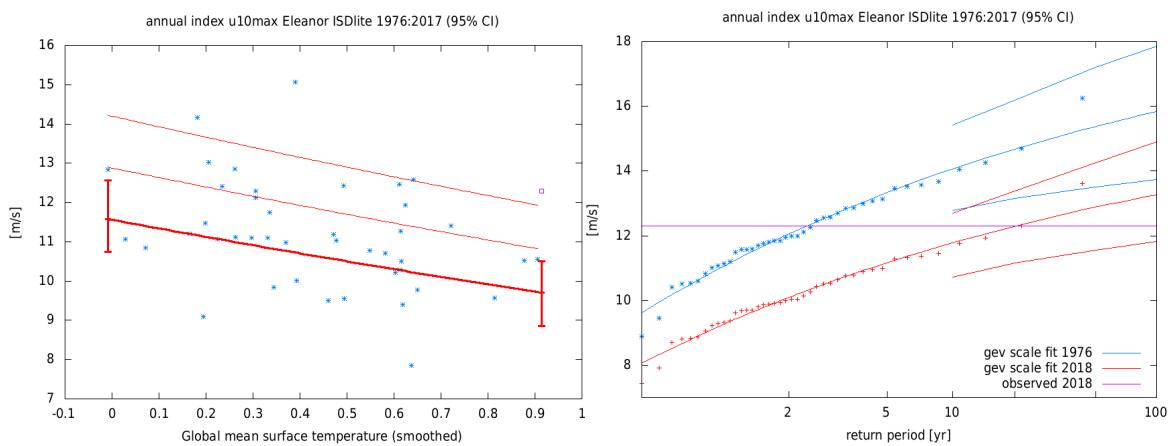
**Figure 9: Same as Figure 4 but for the Eleanor index.**
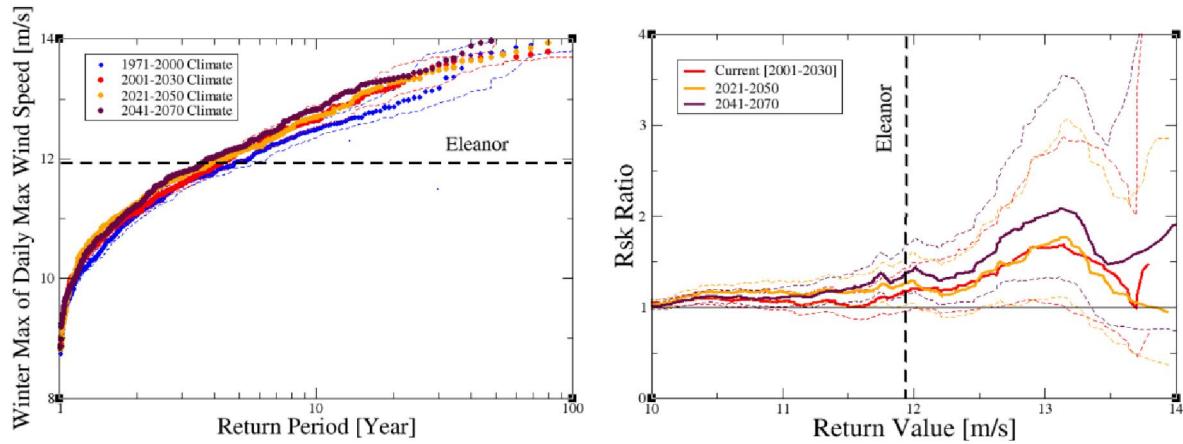
**Figure 10: Same as Figure 5 for Storm Eleanor**
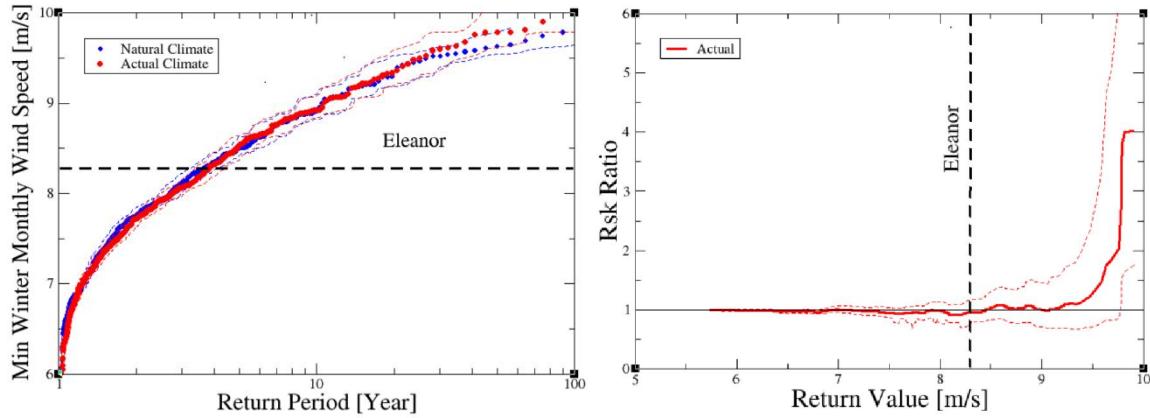
**Figure 11: As for Figure 10 but for the HadGEM3-A ensembles**
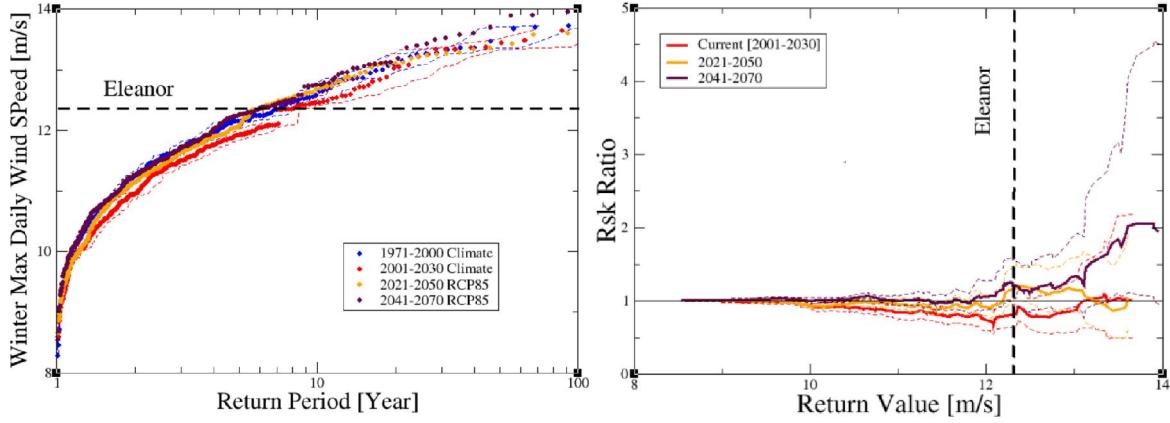
**Figure 12: same as Figure 8 for Storm Eleanor**
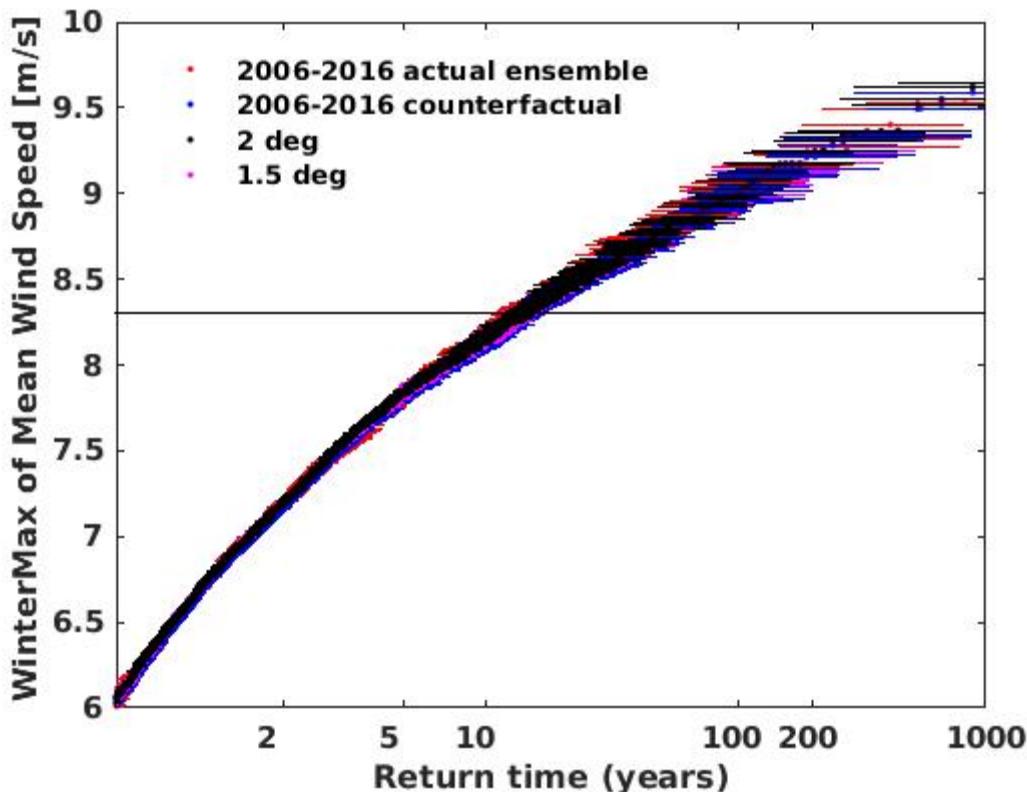
**Fig 13: Return values as a function of return periods for the Storm Eleanor indicator for the weather@home ensemble with 5-95% significance intervals, calculated from a nonparametric bootstrap.**
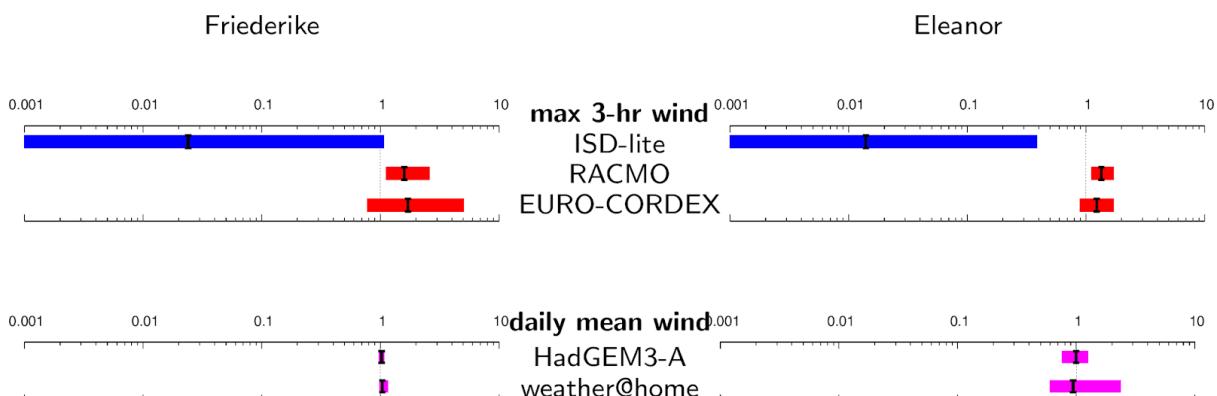
**Figure 14: Synthesis of the probability ratios for storms Friederike and Eleanor. The top comparison is for the daily maximum of 3-hourly instantaneous wind speeds, all probability ratios have been converted to 1975–2055 assuming the logarithm scales with the $CO_2$ concentration. The bottom row shows the two models with daily mean wind speeds, both adjusted to pre-industrial (taken as 1860) to 1.5 ºC (taken as 2055). Top panels are for maximum daily winds from 3-hourly measurements (blue for observations and red for models) and bottom panels for daily mean winds.**

**Tables**

| Model/ensemble [m/s] | WXm *WMm* | WX95 *WM95* | WX99 *WM99* | WXm *WMm* | WX95 *WM95* | WX99 *WM99* |
|---|---|---|---|---|---|---|
| | Friederike | | | Eleanor | | |
| OBS (ISD-Lite) Daily max ** Daily mean | 6.4  *4.5* | 11.4  *8.4* | 13.5  *10.1* | 6.1 [5.8] *4.1* | 9.7 [9.5] *6.6* | 11.1 [11.] *7.7* |
| RACMO (16 members) [Stations] RACMO (16 members) [Area] | 6.8 6.6 | 10.9 10.4 | 12.6 12.0 | 5.3 5.5 | 8.2 8.5 | 9.4 9.8 |
| HADGEM3A*(15mem.) [Stations] HADGEM3A*(15mem.) [Area] | *4.4* *3.9* | *8.1* *7.6* | *9.6* *9.0* | *3.5* *3.1* | *5.7* *5.4* | *6.7* *6.3* |
| bc-EURO-CORDEX(pooled) [St.] bc-EURO-CORDEX(pooled) [Ar.] | 5.9 5.6 | 10.2 9.7 | 12.0 11.5 | 4.7 4.7 | 7.5 7.8 | 8.7 9.1 |
| bc-ARPEGE [zoomed version] | 5.7 | 9.8 | 11.9 | 4.8 | 7.6 | 8.9 |
| bc-RACMO+HADGEM | 6.2 | 10.4 | 12.0 | 4.9 | 7.9 | 9.0 |
| bc-RACMO+ECEARTH | 6.2 | 10.4 | 12.2 | 4.7 | 7.8 | 9.2 |
| bc-REMO+MPI | 6.0 | 10.2 | 12.1 | 4.7 | 7.8 | 9.0 |
| bc-WRF+IPSL | 5.9 | 10.2 | 12.1 | 4.7 | 7.9 | 9.0 |

| | | | | | | |
|---|---|---|---|---|---|---|
| bc-HIRHAM+ECEARTH | 5.8 | 10.2 | 11.8 | 4.7 | 7.8 | 9.2 |
| bc-RCA+ARPEGE | 5.8 | 10.0 | 11.8 | 4.7 | 7.9 | 9.2 |
| bc-RCA+IPSL | 5.8 | 10.0 | 11.7 | 4.7 | 7.8 | 9.2 |
| bc-RCA+HADGEM | 5.7 | 10.1 | 11.6 | 4.7 | 7.9 | 9.2 |
| bc-RCA+MPI | 5.9 | 10.0 | 11.9 | 4.8 | 8.1 | 9.1 |
| bc-RCA+EC-EARTH | 5.6 | 10.0 | 11.8 | 4.5 | 7.8 | 9.0 |
| Weather@Home* | 6.4 | 11 | 11.8 | 5.22 | 8.45 | 9.03 |

**Table 1: Mean, 95th and 99th centiles of the distribution of the daily maxima of wind speed averaged over the 68 stations or the land grid points (for models) for the winter season.**

**(*) Only daily mean winds available, so statistics only from daily means**

**(**) For Eleanor, averages made with stations North of 43.5°N are in brackets**

| Ensemble | Ret. Period yr | PR for Current climate | PR for period 2021-2050 | PR for period 2041-2070 | PR for period PI+1.5°C | PR for period PI+2.0°C |
|---|---|---|---|---|---|---|
| Obs. ISD-Lite | | | N/A | N/A | N/A | N/A |
| *Models using wind speed daily maximum (over 3 hourly data)* | | | | | | |
| RACMO | 15 [11-19] | 1.1[0.8-1.7] | 1.5[1.0-2.2] | 1.5[1.1-2.3] | / | / |
| EURO-CORDEX | 40 [25-80] | 0.9[0.4-2.0] | 1.4[0.7-3.0] | 1.6[0.8-4.1] | / | / |
| *Models using wind speed daily mean* | | | | | | |

| HadGEM3-A | 1.2 [1.15-1.27] | 1.02 [0.98-1.06] | / | / | / | / |
| weather@home | 1.3[1.29-1.35] | 1.03[0.97-0.2] | / | / | 1.039[0.98-1.16] | 1.04[0.98-1.17] |

**Table 2: Event return periods and probability ratios summarized for all model ensembles and for Storm Friederike. Probability ratios (PRs) are calculated with respect to a past or counterfactual period.**

| Ensemble | Ret. Period yr | PR for Current climate | PR for period 2021-2050 | PR for period 2041-2070 | PR for period PI+1.5°C | PR for period PI+2.0°C |
|---|---|---|---|---|---|---|
| Obs. ISD-Lite | | | | | N/A | N/A |
| RACMO | 4.2[3.7-4.8] | 1.2[1.0-1.4] | 1.3[1.0-1.5] | 1.3[1.1-1.6] | / | / |
| HadGEM3-A | 3.9[3.4-4.5] | 1.0[0.8-1.2] | / | / | / | / |
| EURO-CORDEX | 6.6 [5.6-6.9] | 0.8[0.6-1.0] | 1.2[1.-1.4] | 1.2[0.9-1.6] | / | / |
| weather@home | 13.9[13.6-15] | 1.01[0.62-2.35] | / | / | 0.94[0.6-2.35] | 0.94[0.59-2.36] |

**Table 3: Event return periods and probability ratios summarized for all model ensembles and for Storm Eleanor.**